Carbohydrate Polymers 92 (2013) 2002–2011

Contents lists available at SciVerse ScienceDirect

Carbohydrate Polymers

journal homepage: www.elsevier.com/locate/carbpol

Psyllium husk gum: An attractive carbohydrate biopolymer for the production of stable canthaxanthin emulsions

Seyed Mohammad Taghi Gharibzahedi, Seyed Hadi Razavi*, Seyed Mohammad Mousavi

Bioprocess Engineering Laboratory (BPEL), Department of Food Science, Engineering and Technology, Faculty of Agricultural Engineering and Technology, University of Tehran, P.O. Box 4111, Karaj 31587-77871, Iran

ARTICLE INFO

Article history:
Received 8 October 2012
Received in revised form 7 November 2012
Accepted 26 November 2012
Available online 3 December 2012

Keywords:
Emulsion stability
Power ultrasound
Whey protein isolate
Psyllium husk gum
Response surface optimization (RSM)
Canthaxanthin

ABSTRACT

The physical stability of the ultrasonically prepared emulsions containing canthaxanthin (CX) produced by *Dietzia natronolimnaea* HS-1 strain was maximized using a face central composite design (FCCD) of response surface methodology (RSM). The linear and interaction effects of main emulsion components (whey protein isolate (WPI, 0.4–1.2 wt%), psyllium husk gum (PHG, 1.5–4.5 wt%) and coconut oil (CO, 5–10 wt%)) on the stability were studied. The density, turbidity and droplet size of emulsions were also characterized to interpret the stability data. A significant second-order polynomial model was established ($p < 0.0001$). Maximum stability of 98.8% was predicted at the optimum levels of formulation variables (WPI concentration 1.20 wt%, PHG content 3.30 wt%, CO concentration 5.43 wt%). The results also demonstrated that CO and WPI concentration had greater effect on the droplet size and density values, whereas the PHG:WPI ratio had a rather greater effect on the turbidity values.

1. Introduction

The emulsion and colloidal systems are thermodynamically unstable systems and tend to destabilize due to an excess surface free energy, where stability implies no tendency toward structural changes (Gharibzahedi, Mousavi, Hamedi, Khodaiyan, & Razavi, 2012; Sun, Gunasekaran, & Richards, 2007). Emulsion stability is characterized by various mechanisms such as creaming or sedimentation (caused by gravity), flocculation of droplets, coalescence between droplets, Ostwald ripening, and phase inversion (Gharibzahedi, Mousavi, Hamedi, & Ghasemlou, 2012; Harnsilawat, Pongsawatmanit, & McClements, 2006). The stability of emulsions is normally extended by using a combination of various stabilizers and emulsifiers (Huang, Kakuda, & Cui, 2001).

Emulsions stabilized with proteins are more stable than those stabilized with low molecular weight emulsifiers since the proteins can simultaneously anchor onto the dispersed phase on several sites forming thick and flexible film and preventing coalescence of the droplets (Klein, Aserin, Svitov, & Garti, 2010; Rodea-González et al., 2012; Taherian, Britten, Sabik, & Fustier, 2011). Whey protein isolate (WPI) due to its surface-active property has been widely used as an excellent emulsifier in the food industry. This surface-active globular protein rapidly adsorbs at the oil–water interface and provides protection for oil droplets through a combination of electrostatic and steric interactions (Matsumiya, Takahashi, Inoue, & Matsumura, 2010; Sun et al., 2007; Taherian et al., 2011). Polysaccharides are excellent stabilizing agents due to their hydrophilicity, highly branched structure and high molecular weight that impart thickening and gelling characteristics to them. They form a macromolecular barrier against destabilizing mechanisms by increasing the continuous phase viscosity (Sun & Gunasekaran, 2009; Sun et al., 2007).

WPI is widely used in food emulsions in combination with polysaccharides. For example, Sun et al. (2007) found that the addition of xanthan gum (XG) to WPI-stabilized O/W emulsions significantly affected the emulsion microstructure, viscosity, and physicochemical stability. Psyllium seed (*Plantago ovata* Forsk) has been broadly distributed all over the moderate regions of the world, especially in India and Iran (Guo, Cui, Wang, Goff, & Smith, 2009). This seed is utilized in pharmaceutical and food industries as a medicinally bioactive polysaccharide, and constituting the gel and enhancing the consistency and stability, respectively (Ahmadi, Kalbasi-Ashtari, Oromiehie, Yarmand, & Jahandideh, 2012; Bemiller & Whister, 1996; Guo, Cui, Wang, & Young, 2008). Generally, all of these practical specifications attribute to hydrocolloid nature of psyllium husk. Guo et al. (2008) fractionated psyllium husk into three main polysaccharide fractions based on their solubility in water and alkaline solution in order to find a relationship between the structure and its gelling property. They demonstrated that all fractions contained arabinoxylans with various structural features. However, the major fraction with more than 60% in the psyllium husk was alkaline extractable gelling fraction (AEG). This fraction is

* Corresponding author. Tel.: +98 26 3224 8804; fax: +98 26 3224 9453.
E-mail address: srazavi@ut.ac.ir (S.H. Razavi).

0144-8617/$ – see front matter © 2012 Elsevier Ltd. All rights reserved.
http://dx.doi.org/10.1016/j.carbpol.2012.11.083

composed of arabinoxylan with 1 → 3 and 1 → 4 β-D-xylopyranose linkages and is highly branched with short side chains (Guo et al., 2008, 2009).

Strong interest in the functional product market is growing as result of consumer demand for foods that contain some health-promoting components beyond traditional nutrients. Canthaxanthin (CX, β-β′-carotene-4,4′-dione) is an ubiquitous keto-carotene that is of substantial industrial interest because of its widespread applications in nutraceutical, cosmetic, food and feed industries (Gharibzahedi, Razavi, Mousavi, & Moayedi, 2012). Based on the obtained results by many researchers, it proposes that CX as a new functional ingredient can use in the most functional foods and pharmaceuticals to prevent cancer and cardiovascular diseases (Hojjati, Razavi, Rezaei, & Gilani, 2011; Kotake-Nara, Kim, Kobori, Miyashita, & Nagao, 2002; Shih, Chang, Yang, Chou, & Cheng, 2008). Production of these components from biological resources with regarding to restriction of synthetic carotenoids in different industries has recently developed throughout in the world (Hojjati et al., 2011; Nasri Nasrabadi & Razavi, 2010a). Among the introduced sources, the bacterium of *Dietzia natronolimnaea* HS-1 is recognized as a promising producer of natural CX (Khodaiyan, Razavi, & Mousavi, 2008; Nasri Nasrabadi & Razavi, 2010b).

RSM is a collection of mathematical and empirical techniques useful for establishing models, and for optimizing processes even in the presence of complex interactions. It not only determines the interaction between parameters, but also reduces the number of experimental trials, development time and overall cost (Baş & Boyaci, 2007; Muñoz-Celaya et al., 2012).

To the best of our knowledge, there is no specific study on the effect of various concentrations of the selected oil (coconut oil (CO)), WPI and psyllium husk gum (PHG) on the physical stability of OW emulsions containing microbial CX. Therefore, the objective of this study was to assay the effect of three independent variables on stability of these emulsions using a face central composite design (FCCD) of response surface methodology (RSM).

2. Materials and methods

2.1. Materials for the production and analysis of canthaxanthin

The media ingredients for growth of *D. natronolimnaea* HS-1 including D-glucose, yeast extract, peptone, malt extract and agar were purchased from Sigma–Aldrich Co. (USA). Acetonitrile, dichloromethane, and methanol (HPLC grade) were obtained from Merck Chemical Co. (Darmstadt, Germany). The CX standard and pure ethanol (99.9%, v/v) were provided by the Bioprocess Engineering Laboratory (BPEL) (University of Tehran, Iran) and Bidestan Company (Qazvin, Iran), respectively. Beet molasses was purchased from the Qazvin Sugar Industry (Iran).

2.2. Materials for the emulsions preparation

Sodium benzoate was provided by Fars Chemical Industry Co. (Shiraz, Iran) and food grade citric acid (anhydrous) was purchased from Kimia Gharb-Gostar Industry Co. (Kermanshah, Iran). Potassium sorbate was obtained from Chisso Co. (Tokyo, Japan). CO was purchased from local market. It was selected for emulsion production due to high saturated fatty acids and followed by reduction of oxidation problems. The used oil in present study contained the following fatty acids (mol%): 7.9% C8:0, 6.5% C10:0, 45.6% C12:0, 18.3% C14:0, 8.7% C16:0, 2.9% C18:0, 7.1% C18:1 and 1.4% C18:2 as measured by gas chromatography of methyl esters. WPI was provided by MILEI GmbH (Stuttgart, Germany). The psyllium seeds were obtained from the local medical market during January–February, 2012 in a city located in the west of capital Tehran.

2.3. Extraction of psyllium husk gum

PHG solution was extracted and prepared as previously described by Ahmadi et al. (2012), with minor modifications. Briefly, about 10.0 g psyllium seeds sieved and washed with its triple weight of ethanol (96%, w/v) for 20 min under 120 rpm stirring. This method was carried out three times to remove all foreign matter such as stones, hair, dust particles, dirt, and chaff. After removing ethanol and drying the seeds in an oven at 70 °C, to extract the PHG, an electronic stirrer (JJ-1, Changzhou, China) was applied to disperse cleaned seeds in 100 ml distilled water containing 25 mM Ca^{2+} at 75 ± 1 °C for 1.2 h under stirring at 550 rpm constantly. The insoluble non-carbohydrate fractions of psyllium seeds removed by filtration and the dry matter of filtrate (or dry hydrocolloid) were determined (28%). Enough seed used for extracting hydrocolloid needed for preparing the emulsions containing 1.5, 3 and 4.5% (w/v) PHG concentration.

2.4. Canthaxanthin production

The strain of bacterium *D. natronolimnaea* HS-1 (DSM 44860) used in this work was provided by Bioprocess Engineering Laboratory (BPEL), University of Tehran, Iran. It was kept on yeast/malt agar (YMA) plates containing 10 (g/l) D-glucose, 5 (g/l) yeast extract, 5 (g/l) peptone, 3 (g/l) malt extract and 15 (g/l) agar at pH 7.31. Every month, single colonies were transferred to a fresh plate, incubated for 4 days, and then maintained under refrigeration at 0–4 °C. After preparing pre-culture in liquid YM medium (i.e., the above formulation without agar added), the inoculum was transferred into Erlenmeyer flasks containing 40 g/l beet root molasses and 10 g/l yeast extract. Finally, the flasks were incubated in an orbital incubator (model Stuart S150; Staffordshire, UK) at 180 rpm and 28 ± 2 °C for 6 days to produce CX.

2.5. Pigment extraction and analysis

At the appropriate times during the fermentation process, aliquots (10 ml) of cultures were taken from the bioreactor and centrifuged at 7500 × *g* (2–4 °C) for 7.5 min. The produced supernatant was collected. Then, the cell pellets were washed twice with physiological water (NaCl; 9 g/l in deionized water) and centrifuged again. These cells were re-suspended three times in 3 ml of pure ethanol by vortexing for 5 min and centrifuged again to extract the pigment. A water bath (45 °C) was also used to completely extract the pigments (Khodaiyan et al., 2008). The carotenoid extracts subsequently filtered through a 0.2 μm hydrophobic fluorophore membrane (Sigma–Aldrich Co., USA). A Knauer (Berlin, Germany) HPLC system including a k-1001 HPLC pump, a k-1001 solvent organizer, an on-line degasser, a dynamic mixing chamber and a UV–visible detector (K-2600, Knauer, Germany) was used for the determination of individual carotenoids according to the modified method of Razavi, Blanchard, and Marc (2006). According to this method, the separation was performed on a Lichrospher 100 RP-18 silica column (5.0 mm, 250 mm × 4 mm) at 35 °C. The used isocratic mobile phase was acetonitrile/methanol (80:20, v/v) at a flow rate of 2 ml/min. To protect the column, a pre-column of the same material was used. The volume of injected solutions was 10 μl.

2.6. Preparation of emulsion samples

All emulsions containing microbial CX were prepared in two stages. The coarse emulsions were produced by Ultra Turrax (IKA T25 Digital, Germany) in 6000 × *g* for 10 min, and then further emulsified by using an 25 kHz ultrasonic homogenizer (UP200S,

Hielscher Ultrasonics GmbH, Teltow, Germany) equipped with a 13-mm-diameter sonotrode probe made of titanium at a total nominal output power of 200 W. Briefly, 1.5–4.5% dispersions of PHG based on a FCCD were prepared using deionized water at 70 ± 2 °C with continuous mixing using a blender (IKA-WERK, RW 20 DZM, Staufen, Germany) for 15 min. After cooling the dispersions to 20 °C during mixing, sodium azide (0.02 wt%) as a preservative agent and WPI were added. To achieve full hydration, the mixtures were kept at room temperature (23 ± 1 °C) overnight. CO was added to nonpolar CX and ethanol was evaporated by using a Heidolph Laboratory Digital 4010 rotary evaporator (Heidolph Instruments GmbH & Co., Schwabach, Germany). Because of CX negligible solubility at room temperature, it is dissolved in hot CO at a constant ratio of 1:50 to add it to the O/W emulsions. CX is highly susceptible to thermal degradation, for that, the exposure time at high temperatures should be restricted. Authors examined various times and temperatures under vacuum conditions for achieving the lowest oxidation rate. The results showed that temperature of 97 °C and time 7.5 s at vacuum can lead to CX high solubility with ideal oxidation level (Gharibzahedi, Razavi, & Mousavi, 2012). The peroxide value, anisidine value and total oxidation (Totox) value under these conditions were 0.22 mequiv. O_2/kg oil, 0.26 and 0.70, respectively. The dispersion of CX in CO was maintained overnight to rehydrate and then slowly added to the water phase to prepare an initial coarse emulsion. In the next stage, in order to produce the fine-disperse emulsions with small average droplet size and narrow particle-size distribution, the coarse emulsions were sonicated for 4 min.

By holding the vessel in a refrigerated water bath, the difference of temperature from initial coarse emulsions to final emulsion during emulsification was not more than 20 °C. The pH of the emulsions was adjusted to 6.0 using 0.1 M NaOH when required. At least two separate emulsions were prepared for each treatment. The emulsions were stored at 4 °C, and re-equilibrated to room temperature just before analysis.

2.7. Emulsion stability determination

The susceptibility of emulsions to gravitational separation was measured by determining the level of cream layer or sediment phase. For this test, freshly prepared emulsions (15 ml) were transferred into cylindrical tubes and sealed to prevent evaporation. Tubes were stored at 20 °C for 15 days and changes in the height of cream or sediment as emulsion stability index (ESI) were calculated according to the following expression (Gharibzahedi, Mousavi, Khodaiyan, & Hamedi, 2012):

$$\mathrm{ESI}(\%) = 100 \times \frac{H_E - (H_C + H_S)}{H_E} \quad (1)$$

where H_E is percentage of the initial emulsion height, H_S is the height of the sedimentation phase and H_C is the height of the cream layer.

2.8. Particle size analysis

The particle size distribution of emulsions containing CX was determined at room temperature with a laser diffraction particle size analyzer equipped with an accessory Hydro 2000S (Mastersizer 2000, Malvern Instruments Ltd., Worcestershire, UK). Sample analysis was carried out after sample preparation and during storage in duplicate, based on Mie theory (Huang et al., 2001). Size distribution was characterized by volumetric percentage and mean particle diameter obtained by volume-weighted (D_{43}) and surface-weighted (D_{32}) mean diameters of the emulsion droplets, based on the following equations (Gharibzahedi, Mousavi, Hamedi, & Ghasemlou, 2012; Gharibzahedi, Mousavi, Khodaiyan, et al., 2012):

$$D_{43} = \frac{\sum n_i d_i^4}{\sum n_i d_i^3} \quad (2)$$

$$D_{32} = \frac{\sum n_i d_i^3}{\sum n_i d_i^2} \quad (3)$$

where n_i is the number of droplets of radius d_i.

Also, span is a measure of the distribution width of particles in dispersion which can be determined using the following equation (Gharibzahedi, Mousavi, Hamedi, & Khodaiyan, 2011):

$$\mathrm{Span} = \frac{d(\upsilon, 90) - d(\upsilon, 10)}{d(\upsilon, 50)} \quad (4)$$

where $d(\upsilon, 10)$, $d(\upsilon, 50)$, and $d(\upsilon, 90)$ are diameters at 10%, 50%, and 90% cumulative volume, respectively. In other words, $[d(\upsilon, 90) - d(\upsilon, 10)]$ is the range of the data and $d(\upsilon, 0.5)$ is the median diameter.

Moreover, deviation from the median which is an indicative of polydispersity was also reported as uniformity (U) (Samavati, Emam-Djomeh, Mohammadifar, Omid, & Mehdinia, 2011):

$$U = \frac{1}{d(0.5)} \left(\frac{\sum_i V_i |d(0.5 - d_i)|}{\sum_i V_i} \right) \quad (5)$$

where V_i is the volume of the number of particles existing between the two consecutive diameters.

The coalescence rate of the droplets mainly follows first-order kinetics and can be evaluated as (Darling, 1987; Román-Guerrero et al., 2009):

$$\frac{N_t}{N_0} = e^{-K_c t} \quad (6)$$

where N_t is the number concentration of droplets at time t; N_0; the number concentration of freshly formed droplets at time 0; K_c is the first-order rate constant, which is related to the probability of the inter droplet film (interfacial layer) rupturing in time t. The apparent coalescence rate (K_c) was determined by plotting $\ln(N_t/N_0)$ against t. Das & Chattoraj (1982) determined the relative droplet number (N_t/N_0), when the volume of emulsion droplets remains constant (C). The relationship between the emulsion droplet number (N) and the mean volume average droplet diameter, ($D_{30} = \left(\sum n_i d_i^3 / \sum n_i\right)^{1/2}$), is as follows:

$$\frac{4}{3}\pi \left(\frac{D_{30}}{2}\right)^3 N = C \quad (7)$$

Then, the relative number of emulsion droplets can be obtained using equation below (Ruíz-Ramos et al., 2006):

$$\frac{N_t}{N_0} = \left(\frac{(D_{30})_{t=0}}{(D_{30})_{t=t}}\right) \quad (8)$$

2.9. Turbidity measurement

The turbidity of selected emulsions was measured by a UV–vis spectrophotometer (DR/4000U-HACH, USA) after emulsions were aged for 24 h. The samples were diluted with 0.1% solution of sodium dodecyl sulfate (SDS) to a range of different oil droplet concentrations. The diluted emulsions were transferred to a quartz cuvette with a 1 cm path length for the measurement of turbidity at a wavelength of 500 nm. The turbidity was determined based on the below equation (Wang, Wang, Li, Adhikari, & Shi, 2011):

$$T = 2.303 \frac{A \cdot V}{l} \quad (9)$$

where T is the turbidity in (1/m), A is the observed absorbance, V is the dilution factor, and l is the path length of the cuvette (0.01 m).

The turbidity rate constant (k) was also determined by the following equation (Maruyama, Seki, & Satoh, 2012):

$$\ln \frac{T}{T_0} = -Kt \tag{10}$$

where T_0 is the turbidity of emulsion in (1/m) determined immediately after it was prepared and T is the emulsion turbidity in (1/m) at time t, t is time and K is the first-order rate constant.

By plotting time (t) versus $\ln(T/T_0)$, a straight line will be obtained. The K value will be approximated from the slope value of the line.

2.10. Density measurement

The density of the emulsions was measured in triplicate at room temperature (23 ± 1 °C) by a digital densitometer (AP-PAAR DMA 46, Germany) with an accuracy of 10^{-4} g/cm^3. The experiments were carried out in triplicate and the average values were recorded.

2.11. Measurement of the aqueous phase viscosity

Viscosity of the emulsions aqueous phase was measured using a constant stress rheometer (Brookfield DV-II, LV Viscometer, USA) equipped with the ULA spindle, with about 20 ml sample size, at 23 ± 1 °C and different rotational speeds depending on their torque values. After primary experiments, the appropriate torque value was found between 10% and 100% of the measuring range to obtain reliable results. Analyses were performed in triplicate immediately after production of the samples (Gharibzahedi et al., 2011).

2.12. Measurement of canthaxanthin entrapment efficiency

The CX entrapment efficiency of the optimum emulsions was evaluated as described by Yue et al. (2009). Briefly, in a Beckman L8-M Ultracentrifuge (Beckman Instruments Inc., USA), about 3 ml of the emulsion was ultracentrifuged at $162{,}000 \times g$ at 4 °C for 1 h. The entrapment efficiency (EE) of CX was determined by measuring the amount of CX (C_W) in the water layer obtained after ultracentrifugation (UC). The EE was determined using Eq. (11) given below:

$$\text{EE\%} = \left(1 - \frac{C_W}{C_T} \times r\right) \times 100\% \tag{11}$$

where C_T is the concentration of CX and r is the ratio of the aqueous phase volume of the emulsion to the total volume.

2.13. Experimental design and data analysis

The Design Expert Version 7.0 (Minneapolis, MN) software was used to conduct the experimental design for studying the stability of emulsions. RSM-FCCD was applied to determine the influence of three independent variables – WPI concentration (0.4–1.2 wt%, x_1), PHG content (1.5–4.5 wt%, x_2) and CO concentration (5–10 wt%, x_3) – on stability (Y) of the emulsions. The uncoded (actual) and coded levels of the independent variables are illustrated in Table 1. Twenty experiments were augmented with three times and were carried out at the center points to evaluate the pure error (Table 1). The stability was expressed by a second-order polynomial equation as a function of the independent variables as follows:

$$Y = \beta_{k0} + \sum_{i=1}^{4} \beta_{ki} X_i + \sum_{i=1}^{4} \beta_{kii} X_i^2 + \sum_{i<j=2}^{4} \beta_{kij} X_i X_j \tag{12}$$

where Y is the predicted response; β_{k0}, β_{ki}, β_{kii}, and β_{kij} represent regression coefficients; and x_i, X_j are the coded independent factors.

The quality of the polynomial model fit was expressed by the coefficients of determination R^2 and adjusted R^2 (R^2_{adj}). Adequate precision (AP) compares the range of the predicted values at the design points to the average prediction error. AP is defined in Eq. (13) (Baş & Boyaci, 2007):

$$\text{AP} = \frac{\max(\bar{y}) - \min(\bar{y})}{\sqrt{p\sigma^2/n}} \tag{13}$$

In Eq. (13), $\bar{y}$ is the predicted value, p is the number of model parameters, σ^2 is the residual mean square from ANOVA table, and n is the number of experiments.

The significances of each of the coefficients in the empirical model were selected or rejected based on the p-value. The terms statistically found non-significant ($p > 0.05$) were removed from the initial models and the experimental data were refitted to only the significant ($p < 0.05$) factors to produce the final reduced model. It should be noted that some non-significant variables ($p < 0.05$) were added again to the model due to quadratic or interaction effects. For the graphical analysis of the independent variable interactions, the use of 3D surface and counter plots of the regression models was highly recommended (Gharibzahedi, Mousavi, Hamedi, & Ghasemlou, 2012). Thus, these plots were depicted from the fitted polynomial equation to explain the interactive effects of the independent variables with the response variable.

Moreover, the data of droplet size characteristics, turbidity and density of emulsions in order to interpret the results obtained on emulsion stability were subjected to analysis of variance (ANOVA), applying randomized complete block design, and Fisher's least significant difference (LSD) test using SPSS 13 (SPSS Inc., USA) software.

3. Results and discussion

3.1. Preliminary investigation

Preliminary experiments were carried out to determine the effect of various operating conditions in the ultrasonic emulsification (applied power, ultrasound frequency and process time) on the particle size and also the best preparation conditions to obtain a small mean particle size (0.759 ± 0.102 μm) and narrow size distribution. The results revealed that fine emulsification by ultrasonic treatment obtained at applied power 200 W, frequency 25 kH and running time 115 s (data not shown) as similar results reported by Jafari, He, and Bhandari (2007) and Farzi, Saffari, Emam-Djomeh, and Mohammadifar (2011) for sub-micron emulsions and gum tragacanth dispersions produced by ultrasound technique. It seems that the above conditions can lead to the significant disruption of large particles, resulting in smaller particles with a narrower particle size distribution.

3.2. Fitting the response surface model

A multiple regression analysis was carried out using RSM-FCCD to (I) fit mathematical models to the experimental data aiming at a maximum level for the response variable studied; (II) define the relationship between three independent variables and the response variable as shown in Table 1. Fitting of the data to different models and their subsequent ANOVA demonstrated that the emulsion stability was best described with a second-order polynomial model as follows:

$$Y = 93.99 + 3.40X_1 + 0.95X_2 - 1.70X_3 + 0.99X_1^2 - 2.85X_2^2 - 0.90X_3^2 - 0.82X_1X_2 + 0.37X_1X_3 - 0.35X_2X_3 \tag{14}$$

Table 1
Experimental design and results for stability of emulsions containing bacterial CX.

Run	Independent variables			Emulsion stability (%)	
	X_1[a]	X_2[b]	X_3[c]	Experimental[d]	Predicted
1	0.4 (−1)	1.5 (−1)	5.0 (−1)	88.2 ± 0.1	88.2
2	1.2 (1)	1.5 (−1)	5.0 (−1)	95.0 ± 0.1	95.1
3	0.4 (−1)	4.5 (1)	5.0 (−1)	91.7 ± 0.2	91.6
4	1.2 (1)	4.5 (1)	5.0 (−1)	96.8 ± 0.0	96.8
5	0.4 (−1)	1.5 (−1)	10.0 (1)	84.0 ± 0.0	83.9
6	1.2 (1)	1.5 (−1)	10.0 (1)	93.9 ± 0.1	93.9
7	0.4 (−1)	4.5 (1)	10.0 (1)	87.7 ± 0.2	87.6
8	1.2 (1)	4.5 (1)	10.0 (1)	92.7 ± 0.2	92.7
9	0.8 (0)	3.0 (0)	7.5 (0)	94.5 ± 0.3	94.4
10	0.8 (0)	3.0 (0)	7.5 (0)	94.3 ± 0.2	94.4
11	0.8 (0)	3.0 (0)	7.5 (0)	93.5 ± 0.3	93.6
12	0.8 (0)	3.0 (0)	7.5 (0)	93.9 ± 0.3	93.6
13	0.4 (−1)	3.0 (0)	7.5 (0)	91.4 ± 0.2	91.5
14	1.2 (1)	3.0 (0)	7.5 (0)	98.6 ± 0.0	98.3
15	0.8 (0)	1.5 (−1)	7.5 (0)	90.3 ± 04	90.1
16	0.8 (0)	4.5 (1)	7.5 (0)	92.0 ± 0.5	92.0
17	0.8 (0)	3.0 (0)	5.0 (−1)	94.9 ± 0.0	94.7
18	0.8 (0)	3.0 (0)	10.0 (1)	91.3 ± 0.1	91.3
19	0.8 (0)	3.0 (0)	7.5 (0)	93.2 ± 0.4	93.9
20	0.8 (0)	3.0 (0)	7.5 (0)	94.3 ± 0.0	93.9

[a] WPI concentration.
[b] PHG content.
[c] CO concentration.
[d] Mean ± standard deviation (n = 3).

The ANOVA of the second-order regression model indicated that the stability model was highly significant, as was evident from the F-test with a very low probability value ($p < 0.0001$) (Table 2). The predicted values of emulsion stability were calculated using the regression model and compared with experimental values in Table 1. The lack of fit value of the model was 0.9324 (Table 2), which implied that it was not significant relative to the pure error (Gharibzahedi, Mousavi, Khodaiyan, et al., 2012). The total determination coefficient (R^2) was 0.995, proving a reasonable fit of the model to experimental data. The adjusted R^2 value (0.989%) also indicates the precision of the model (Table 2). Adjusted R^2 is a modification of R^2 that adjusts for the number of explanatory terms in a model. At the same time, the CV value was 0.37%, indicating high degree of precision and reliability of the experimental values (Table 2). The AP measures the signal-to-noise ratio, with a ratio greater than 4 being desirable (Gharibzahedi, Mousavi, Hamedi, & Ghasemlou, 2012). The AP of 53.44 indicated that this model could be used to navigate the design space.

3.3. Emulsion stability

Table 2 illustrates that, among the three independent variables, WPI concentration exerted the highest significance on the stability value ($p < 0.0001$; SS = 115.60) followed by CO concentration ($p < 0.0001$; SS = 28.90) and PHG content ($p < 0.0001$, SS = 9.02). Also, the quadratic and interaction terms of PHG content, CO concentration and WPI concentration were highly significant.

Fig. 1 shows that the relationship between the interaction effect of independent variables and the stability value was strongly nonlinear in the investigated independent variable ranges. Fig. 1A and B shows the effect of PHG and WPI concentration on the stability of emulsions. As illustrated, when the PHG content increased from 1.5 to 3.1%, the stability increased from 88.9 to more 96%. The results also showed that the aqueous phase viscosity of the emulsions containing 1.2 wt% WPI and 5.0 wt% CO increased from 22 to 0.68 Pa s with increasing concentrations of PHG at a constant shear rate of 50 s^{-1}. Morris (1990) showed that weak polysaccharide gel

Table 2
Analysis of variance of the experimental results of the RSM-FCCD.

Source	Sum of squares (SS)	df[a]	Mean of squares	F-value	Probability > F[b,c]
Model	197.37	9	21.93	182.36	<0.0001**
X_1 (WPI concentration)	115.60	1	115.60	961.27	<0.0001**
X_2 (PHG content)	9.02	1	9.02	75.04	<0.0001**
X_3 (CO concentration)	28.90	1	28.90	240.31	<0.0001**
X_{11}	2.67	1	2.67	22.27	0.0015**
X_{22}	21.81	1	21.81	181.42	<0.0001**
X_{33}	2.17	1	2.17	18.12	0.0028**
X_{12}	5.44	1	5.44	45.27	0.0001**
X_{13}	1.12	1	1.12	9.35	0.0156*
X_{23}	0.98	1	0.98	8.14	0.0213*
Residual	0.96	8	0.12	–	–
Lack of fit	0.25	5	0.051	0.218	0.9324
Pure error	0.70	3	0.23	–	–
Core total	205.55	19	–	–	–

R^2 = 0.995; adjusted-R^2 = 0.989; CV = 0.37; adequate precision (AP) = 53.44

[a] Degree of freedom.
[b] Significant (*$p < 0.05$).
[c] Highly significant (**$p < 0.01$).

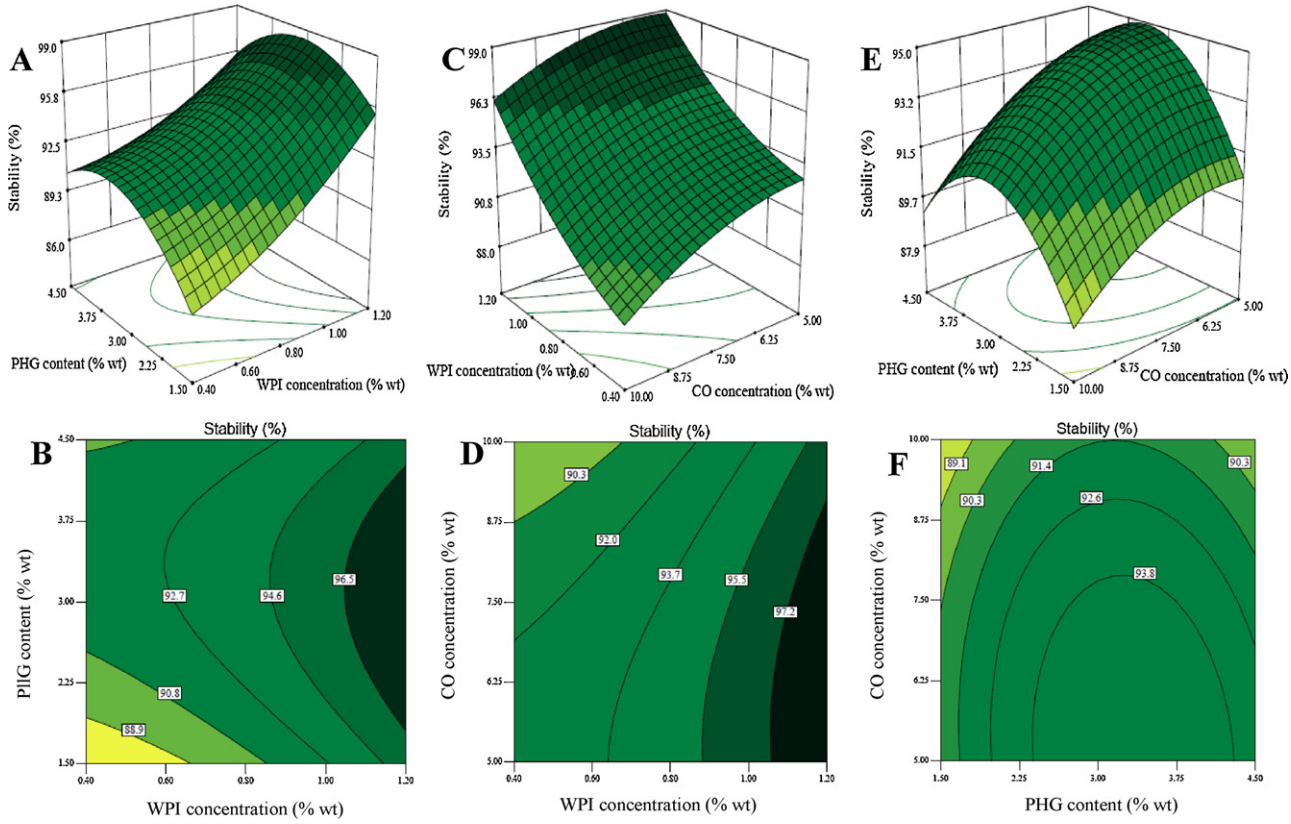

Fig. 1. Response surface plots (A–C) and contour plots (D–F) showing the effect of WPI concentration (X_1), PHG content (X_2) and CO concentration (X_3) on the emulsion stability.

of PHG in different solutions is formed by overlapping and entangled flexible random coil chains. Guo et al. (2008) reported PHG has high molecular weight and can be expected to be good viscosity enhancer. It was also demonstrated that the high viscosity in solutions containing high amounts of PHG is due to the presence of an arabinoxylan with 1 → 4 linkages in the xylan backbone in AEG faction of PHG structure which was heavily substituted by short arabinose branches (An, Wang, & Wang, 2010; Fischer et al., 2004; Guo et al., 2008). Guo et al. (2008) pointed out that the behavior of AEG as a rigid chain is also because of large mean hydrodynamic diameter (>100 nm) of this fraction. Therefore, in high concentration of PHG, network structure formation in the emulsion droplets by increasing the viscosity of the continuous phase slows down the mobility of droplets leaving enough time for the emulsifier to adsorb at the O/W interface and therefore stabilizes the oil droplets against coalescence. However, PHG had a negative effect at higher concentrations of 3.62% on the stability of O/W emulsions enriched with CX (Fig. 1A and E). Fast instability occurred when a critical PHG concentration (3.62 wt%) was exceeded, which was attributed to depletion flocculation of the droplets by the non-adsorbed PHG molecules in the aqueous phase of the emulsions. Non-adsorbed polymers at high concentration of PHG lead to an attractive osmotic force between droplets that enhance as the polymer concentration increases, until finally it becomes large enough to overcome the repulsive forces acting between the droplets. This fact causes an increase in the bulk viscosity of the system. Gunning, Hibberd, Howe, and Robins (1988) attributed the emulsion destabilization by high XG contents to depletion flocculation since they found no evidence for adsorption of XG at the emulsion droplet surface. These results were also in agreement with those of Klinkesorn, Sophanodora, Chinachoti, and McClements (2004), who found that excessive concentrations of maltodextrin in corn oil-in-water emulsions due to depletion flocculation cause to enhance the instability rate. Thus, a droplet network structure formed in the emulsions with PHG optimal contents and the suitable viscosity of the aqueous phase delayed the instability. Moreover, the existence of Ca^{2+} ions in PHG solution can also increase in the density of aggregates, and thus the polymer network became stronger. It might be attributed to the fact that these ions promote aggregation of AEG fraction by directly interacting with the polysaccharide chains, or by changing the conformation of the polysaccharide strands to favor the association process encouraging aggregation (Guo et al., 2009).

Also, the results clearly showed that PHG alone is unable to form very stable emulsions containing bacterial CX. The stability of emulsions was higher as mixed with WPI in suitable ratios. Laplante, Turgeon, and Paquin (2005) and, Klaypradit & Huang (2008) have reported similar results in the case of O/W emulsions stabilized by WPI with XG or chitosan (CS). Taherian et al. (2011) also found that O/W emulsions produced with conjugated WPI-fish gelatin (FG) generated higher viscosity, elasticity, and stability compare to those produced with WPI or FG alone. This fact might be attributed to diluting WPI coated droplets in hydrated FG increase the interfacial film viscosity and elasticity because of the interactions between WPI and FG on the droplets surface of double coated emulsions resulting in better stability (Fitzsimons, Mulvihill, & Morris, 2008; Taherian et al., 2011). In contrast, as demonstrated by the data depicted in Fig. 2A, the emulsions prepared with WPI without PHG indicated a considerable instability due to polysaccharides providing polymeric steric hindrance to the oil droplets and oil droplets becoming entrapped in the network formed by the polysaccharides (Laplante et al., 2005). The results also agree with those found

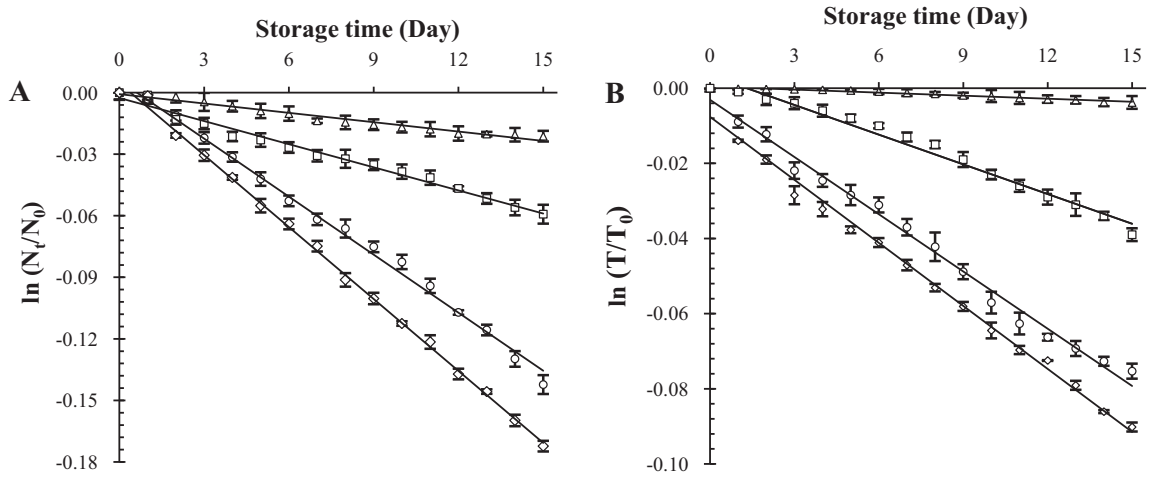

Fig. 2. Kinetic plots of $\ln(N_t/N_0)$ versus storage time (A) and of $\ln(T/T_0)$ versus storage time (B) for the canthaxanthin emulsions containing different contents of PHG: 0 wt% (◊),1.5 wt% (□), 3.0 wt% (△) and 4.5 wt% (○) and the same concentrations of WPI (=1.2 wt%) and CO (=5.43 wt%).

by Samavati, Emam-Djomeh, Mohammadifar, Omid, and Mehdinia (2012). They observed a high creaming index in the emulsions comprising WPI without XG.

From the optimization results, an emulsion containing 1.20 wt% WPI, 3.30 wt% PHG and 5.43 wt% CO was predicted to be the individual optimum region that resulted in highest emulsion stability (98.80%). Nevertheless, the least emulsion stability (84.30%) was estimated to be at the combined level of 0.4 wt% WPI, 1.5 wt% PHG and 10 wt% CO. Fig. 2A shows the kinetic plots of $\ln(N_t/N_0)$ versus storage time as a function of the PHG content in the emulsions. There were significant differences ($p < 0.05$) among coalescence rates of emulsions with different PHG concentrations. The results showed that the emulsion with similar formulation to the optimum sample had the least instability rate during storage period (Fig. 2A).

Fig. 1A–D depicts the stability of emulsions increased substantially with increased proportions of WPI. An increase in WPI concentration during emulsion formation enhanced adsorption of the protein molecules and surface coverage of oil droplets, against flocculation and reduced the scope for WPI bridging, leading to decreased creaming (Sun & Gunasekaran, 2009; Samavati et al., 2012). As considered in Fig. 3, increases in WPI concentration resulted in reduced droplet size (D_{43} and D_{32}), although droplet size increased significantly with increased CO concentration. Fig. 1C–F illustrates that the emulsion stability reduced sharply with increased CO concentration. Buffo, Reineccius, and Oehlert (2001) also found that when the oil-phase content is increased, the oil-droplet coverage is reduced and, consequently, the stability of the emulsion is reduced. Sun et al. (2007) explained that increasing oil phase volume fraction increased the flocculation rate due to collision frequency among oil droplets.

The ANOVA results indicated that span and uniformity characteristics were mainly influenced by WPI and CO concentrations and to a less extent by PHG content (data not shown). Comparing the polydispersity indices of emulsions containing the various concentrations of CO and WPI demonstrated that these values were significantly greater for all of the recipes having high CO/WPI ratio (Fig. 4). Gharibzahedi, Mousavi, Hamedi, and Ghasemlou (2012) also found that an increase in the emulsifier content and initial concentration of the applied oil were associated with high emulsion stability and minimum droplet size along with narrow size distribution. As clearly shown in Fig. 3, there was no significant effect of PHG content on the D_{43} and D_{32} of the emulsions. These findings confirm the lack of interactions between PHG and WPI-coated droplets and no adsorption of polysaccharides on the surface of the oil droplet. pH usually is one of the most important factors in the complexation between two charged biopolymers. PHG is an anionic polysaccharide that bears a negative charge due to ionized carboxyl groups (Ahmadi et al., 2012). WPI is also composed of a mixture of β-lactoglobulin, α-lactalbumin, bovine serum albumin, and other proteins such as caseins. The proteins in WPI have isoelectric points (p*I*) around pH 5. At pHs lower than 5, the solubility due to the neutralization of charge on the WPI molecules decreased. However, these molecules have a negative charge at pH greater than their pI (Klein et al., 2010). Therefore, the protein-coated droplets and polysaccharide molecules during complexation at relatively high pH values were both strongly negatively charged and so no adsorption occurred (Guzey & McClements, 2007). Sila et al. (2009) showed that the electrical charge on biopolymers may also be changed by their interactions with other ionic species in the environment. These interactions typically involve multivalent ions such as calcium that bind to oppositely charged groups on the biopolymer chain, altering overall charge characteristics. The presence of Ca^{2+} ions in PHG solution can covalently form cross-links between free carboxyl and amino groups along neighboring polymer chains and can cause a decrease in negative charge. Therefore, adding Ca^{2+} ions resulted in an increase in the density of aggregates, and the network became stronger.

The results obtained from the turbidity determination indicated a more complex dependence on PHG:WPI ratio in the emulsions (Fig. 5). An interest increase in the turbidity amount was observed when this ratio was augmented from 1.25 (treatment nos. 2 and 6) to 2.5 (treatment no. 14). As considered in Table 2, sample no. 14 had the highest stability (98.3%) among the emulsions investigated. A further increase of this ratio from 2.5 to 11.25 led to a decrease in the turbidity rate and an increase in polydispersity and heterogeneity of the emulsions. Harnsilawat et al. (2006) pointed out that the turbidity of an emulsion can reflect its stability due to its dependence to the droplet size and concentration. Since the larger droplets scatter light less effectively than smaller ones, the emulsion may appear less turbid. Figs. 3C, F and 4A confirmed that the emulsions containing 3.0% PHG and 1.2% WPI had the lowest droplet size and particle size distribution. The data obtained in this study for the loss rate of turbidity indicated that the emulsions turbidity decreased during storage. The lower degree of turbidity loss rate indicates more cloud stability in oil-in water emulsions (Gharibzahedi, Mousavi, Hamedi, & Ghasemlou, 2012). Fig. 2B shows that the value of turbidity rate constant at the optimum levels of CO and WPI decreased significantly with

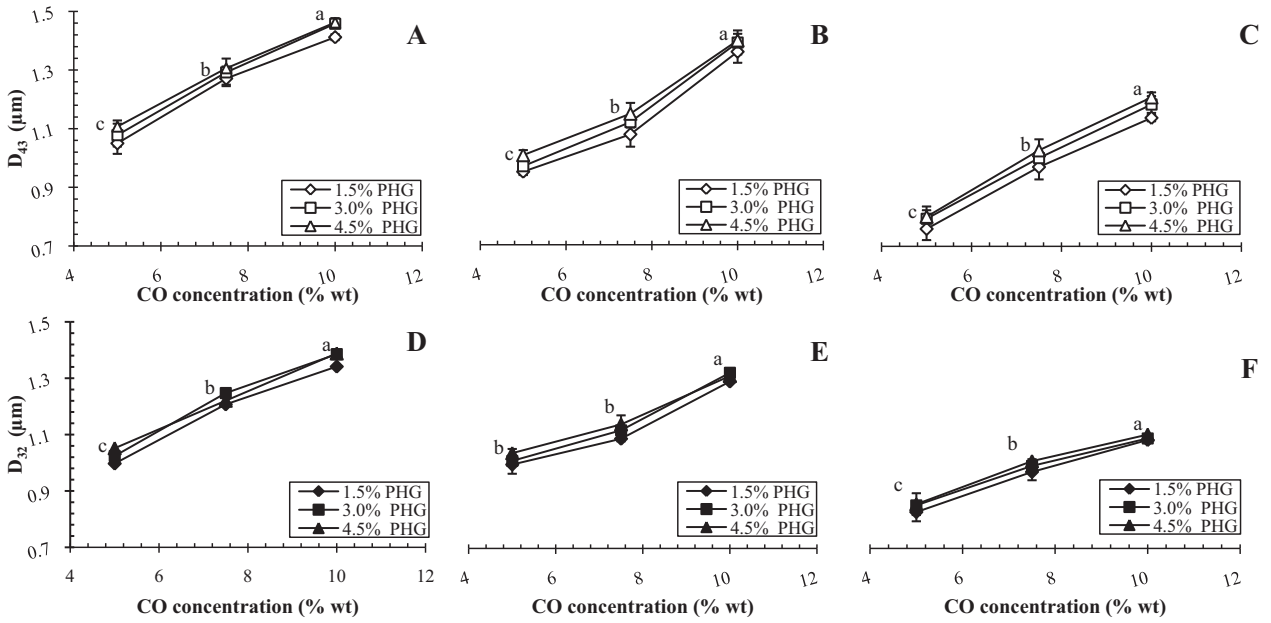

Fig. 3. Changes in D_{43} (A–C) and D_{32} (D–F) of the emulsions prepared with the various concentrations of CO, PHG and WPI (0.4% (A and D), 0.8% (B and E) and 1.2% (C and F)). Data points represent means ($n = 3$) ± standard deviations. Some error bars lie within the data points. Means with same letters (a–c) are not significantly different ($p < 0.05$).

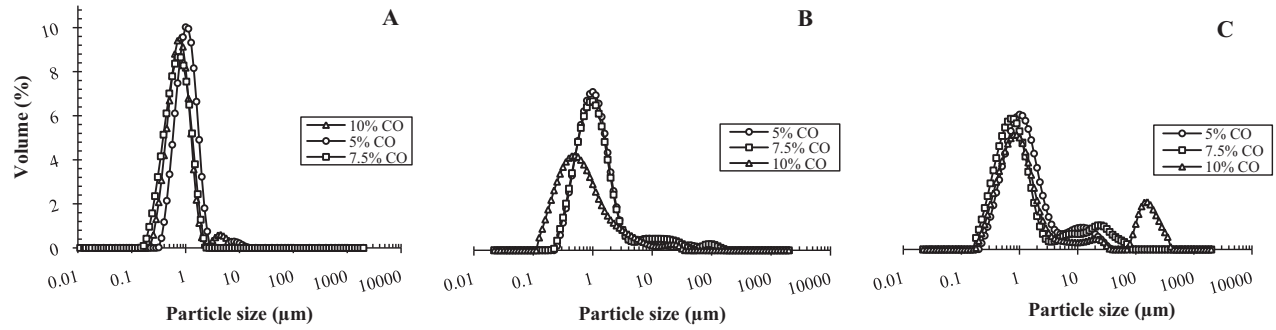

Fig. 4. Droplet size distribution of the emulsions as functions of WPI ((A) 1.2 wt%; (B) 0.8 wt%; (C) 0.4 wt%) and CO concentration values at the same content of PHG (=3.0 wt%).

increasing PHG concentration from 0 to 3%, but increased gradually at higher PHG concentrations. The slope of emulsion with 4.5% PHG was measured at $-0.0026\ d^{-1}$ level while those of 1.5 and 3.0% were obtained at -0.0051 and $-0.0003\ d^{-1}$ levels. The droplets coalescence at high PHG concentrations could be attributed to the strong depletion attraction between the droplets during storage period.

The results revealed also that PHG content compared to WPI and CO concentration had a more significant effect on density of the studied emulsions. A small increase in density value was observed for the emulsions with high WPI and low CO content ($1.0481–1.0532\ g/cm^3$). A possible reason is that increasing WPI concentration would facilitate relatively smaller droplets adsorbing more WPI at the interface of the oil droplets; this would increase the density of droplets and, consequently, decrease the instability rate. Moreover, the density reduction by increasing CO concentration may be explained by the negative effect of the oil phase on the density value (Chanamai & McClements, 2000; Gharibzahedi et al., 2011).

3.4. Validation tests

In order to verify the model prediction, emulsions were produced by repeating four additional experiments under the optimum conditions. The maximum stability found to be 98.62 ± 0.32%, which was clearly very close to the predicted value. Also, the EE of CX in these emulsions was at 93.15 ± 1.09%. These results well agreed with theoretical data predicted by the optimization response model.

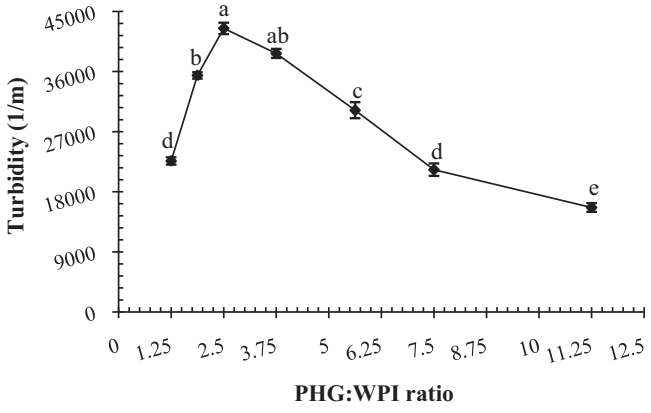

Fig. 5. Effect of PHG:WPI ratio on turbidity of the prepared emulsions at the same concentration of CO (=7.50 wt%).

4. Conclusion

The findings from this study could provide interesting information about the behavior of PHG when mixed with WPI-coated emulsions in presence of bacterial CX as a functional ingredient and will facilitate their application in food systems. In this study, A FCCD-RSM was used to determine the optimum formulation for production of a stable O/W emulsion containing CX biosynthesized by *D. natronolimnaea* HS-1 using 25 kHz ultrasonic emulsification. It was evident that the second-order polynomial model was adequate to describe and predict the emulsion stability. The model had a regression coefficient R^2 of 99.5% whereas the adjusted R^2 was 98.9% indicating the reliability of the model. The most suitable combination of variables for the higher stability (98.8%) was 1.20 wt%, 3.30 wt% and 5.43 wt% for WPI, PHG and CO concentrations, respectively. Emulsion stability in the mixed systems was considerably higher than individual WPI solutions indicating improved ability to stabilize the oil-in-water interface. Rapid instability was obtained when the PHG content exceeded an optimum value, which was attributed to depletion flocculation mechanism caused by the non-adsorbed PHG. Study of the coalescence and turbidity kinetics of the different formulations also confirmed the results predicted by the RSM model. At these optimal conditions, the emulsion stability and the EE of CX were 93.15% and 98.62%, respectively. Thus, this methodology can be applied in the emulsion making process of bioactive compounds in bio industries.

Acknowledgements

The authors would like to extend their appreciation for the financial support provided by the *University of Tehran* and *ZamZam Iran Co*. for its technical and financial assistance.

References

Ahmadi, R., Kalbasi-Ashtari, A., Oromiehie, A., Yarmand, M. S., & Jahandideh, F. (2012). Development and characterization of a novel biodegradable edible film obtained from psyllium seed (*Plantago ovata* Forsk). *Journal of Food Engineering*, *109*, 745–751.

An, J. K., Wang, W. B., & Wang, A. Q. (2010). Preparation and swelling properties of a pH-sensitive superabsorbent hydrogel based on psyllium gum. *Starch/Stärke*, *62*, 501–507.

Baş, D., & Boyaci, I. H. (2007). Modeling and optimization I: Usability of response surface methodology. *Journal of Food Engineering*, *78*(3), 836–845.

Bemiller, J. N., & Whister, R. L. (1996). Carbohydrate. In O. R. Fennema (Ed.), *Food chemistry* (pp. 157–223). New York: Marcel Dekker.

Buffo, R. A., Reineccius, G. A., & Oehlert, G. W. (2001). Factors affecting the emulsifying and rheological properties of gum acacia in beverage emulsions. *Food Hydrocolloids*, *15*, 53–66.

Chanamai, R., & McClements, D. J. (2000). Impact of weighting agents and sucrose on gravitational separation of beverage emulsions. *Journal of Agricultural and Food Chemistry*, *48*, 5561–5565.

Darling, D. F. (1987). Kinetic aspects of food emulsion behaviour. In J. M. V. Blanshard, & P. Lillford (Eds.), *Food structure and behaviour* (pp. 107–145). London: Academic Press.

Das, K. P., & Chattoraj, D. K. (1982). Kinetics of coalescence of polar oil/water emulsions stabilized by ionic detergents and proteins. *Colloids and Surfaces*, *5*, 75–78.

Farzi, M., Saffari, M. M., Emam-Djomeh, Z., & Mohammadifar, M. A. (2011). Effect of ultrasonic treatment on the rheological properties and particle size of gum tragacanth dispersions from different species. *International Journal of Food Science and Technology*, *46*, 849–854.

Fischer, M. H., Yu, N., Gray, G. R., Ralph, J., Anderson, L., & Marlett, J. A. (2004). The gel-forming polysaccharide of psyllium husk (*Plantago ovata* Forsk). *Carbohydrate Research*, *339*(11), 2009–2017.

Fitzsimons, S. M., Mulvihill, D. M., & Morris, E. R. (2008). Segregative interactions between gelatin and polymerised whey protein. *Food Hydrocolloids*, *22*, 485–491.

Gharibzahedi, S. M. T., Mousavi, S. M., Hamedi, M., & Ghasemlou, M. (2012). Response surface modeling for optimization of formulation variables and physical stability assessment of walnut oil-in-water beverage emulsions. *Food Hydrocolloids*, *26*, 293–301.

Gharibzahedi, S. M. T., Mousavi, S. M., Hamedi, M., & Khodaiyan, F. (2011). Application of response surface modeling to optimize critical structural components of walnut–beverage emulsion with respect to analysis of the physicochemical aspects. *Food and Bioprocess Technology*, http://dx.doi.org/10.1007/s11947-011-0763-8

Gharibzahedi, S. M. T., Mousavi, S. M., Hamedi, M., Khodaiyan, F., & Razavi, S. H. (2012). Development of an optimal formulation for oxidative stability of walnut-beverage emulsions based on gum arabic and xanthan gum using response surface methodology. *Carbohydrate Polymers*, *87*, 1611–1619.

Gharibzahedi, S. M. T., Mousavi, S. M., Khodaiyan, F., & Hamedi, M. (2012). Optimization and characterization of walnut beverage emulsions in relation to their composition and structure. *International Journal of Biological Macromolecules*, *50*, 376–384.

Gharibzahedi, S. M. T., Razavi, S. H., & Mousavi, S. M. (2012). Developing an emulsion model system containing canthaxanthin biosynthesized by *Dietzia natronolimnaea* HS-1. *International Journal of Biological Macromolecules*, *51*, 618–626.

Gharibzahedi, S. M. T., Razavi, S. H., Mousavi, S. M., & Moayedi, V. (2012). High efficiency canthaxanthin production by a novel mutant isolated from *Dietzia natronolimnaea* HS-1 using central composite design analysis. *Industrial Crops and Products*, *40*, 345–354.

Gunning, P. A., Hibberd, D. J., Howe, A. M., & Robins, M. M. (1988). Gravitational destabilization of emulsions flocculated by non-adsorbed xanthan. *Food Hydrocolloids*, *2*(2), 119–129.

Guo, Q., Cui, S. W., Wang, Q., Goff, H. D., & Smith, A. (2009). Microstructure and rheological properties of psyllium polysaccharide gel. *Food Hydrocolloids*, *23*, 1542–1547.

Guo, Q., Cui, S. W., Wang, Q., & Young, J. C. (2008). Fractionation and physicochemical characterization of psyllium gum. *Carbohydrate Polymers*, *73*, 35–43.

Guzey, D., & McClements, D. J. (2007). Impact of electrostatic interactions on formation and stability of emulsions containing oil droplets coated by β-lactoglobulin–pectin complexes. *Journal of Agricultural and Food Chemistry*, *55*, 475–485.

Harnsilawat, T., Pongsawatmanit, R., & McClements, D. J. (2006). Stabilization of model beverage cloud emulsions using protein–polysaccharide electrostatic complexes formed at the oil–water interface. *Journal of Agricultural and Food Chemistry*, *54*, 5540–5547.

Hojjati, M., Razavi, S. H., Rezaei, K., & Gilani, K. (2011). Spray drying microencapsulation of natural canthaxantin using soluble soybean polysaccharide as a carrier. *Food Science and Biotechnology*, *20*(1), 63–69.

Huang, X., Kakuda, Y., & Cui, W. (2001). Hydrocolloids in emulsions: Particle size distribution and interfacial activity. *Food Hydrocolloids*, *15*, 533–542.

Jafari, S. M., He, Y., & Bhandari, B. (2007). Production of sub-micron emulsions by ultrasound and microfluidization techniques. *Journal of Food Engineering*, *82*, 478–488.

Khodaiyan, F., Razavi, S. H., & Mousavi, S. M. (2008). Optimization of canthaxanthin production by *Dietzia natronolimnaea* HS-1 from cheese whey using statistical experimental methods. *Biochemical Engineering Journal*, *40*, 415–422.

Klaypradit, W., & Huang, Y. W. (2008). Fish oil encapsulation with chitosan using ultrasonic atomizer. *LWT – Food Science and Technology*, *41*, 1133–1139.

Klein, M., Aserin, A., Svitov, I., & Garti, N. (2010). Enhanced stabilization of cloudy emulsions with gum arabic and whey protein isolate. *Colloids and Surfaces B: Biointerfaces*, *77*(1), 75–81.

Klinkesorn, U., Sophanodora, P., Chinachoti, P., & McClements, D. J. (2004). Stability and rheology of corn oil-in-water emulsions containing maltodextrin. *Food Research International*, *37*, 851–859.

Kotake-Nara, E., Kim, S. J., Kobori, M., Miyashita, K., & Nagao, A. (2002). Acycloretinoic acid induces apoptosis in human prostate cancer cells. *Anticancer Research*, *22*, 689–695.

Laplante, S., Turgeon, S. L., & Paquin, P. (2005). Emulsion stabilizing properties of various chitosans in the presence of whey protein isolate. *Carbohydrate Polymers*, *59*(4), 425–434.

Maruyama, H., Seki, H., & Satoh, Y. (2012). Removal kinetic model of oil droplet from o/w emulsion by adding methylated milk casein in flotation. *Water Research*, *46*, 3094–3100.

Matsumiya, K., Takahashi, W., Inoue, T., & Matsumura, Y. (2010). Effects of bacteriostatic emulsifiers on stability of milk-based emulsions. *Journal of Food Engineering*, *96*, 185–191.

Morris, E. R. (1990). Shear-thinning of 'random coil' polysaccharides: Characterisation by two parameters from a simple linear plot. *Carbohydrate Polymers*, *13*(1), 85–96.

Muñoz-Celaya, A. L., Ortiz-García, M., Vernon-Carter, E. J., Jauregui-Rincón, J., Galindo, E., & Serrano-Carreón, L. (2012). Spray-drying microencapsulation of Trichoderma harzianum conidias in carbohydrate polymers matrices. *Carbohydrate Polymers*, *88*(4), 1141–1148.

Nasri Nasrabadi, M. R., & Razavi, S. H. (2010a). Enhancement of canthaxanthin production from *Dietzia natronolimnaea* HS-1 in a fed-batch process using trace elements and statistical methods. *Brazilian Journal of Chemical Engineering*, *27*(4), 517–529.

Nasri Nasrabadi, M. R., & Razavi, S. H. (2010b). Use of response surface methodology in a fed-batch process for optimization of tricarboxylic acid cycle intermediates to achieve high levels of canthaxanthin from *Dietzia natronolimnaea* HS-1. *Journal of Bioscience and Bioengineering*, *109*, 361–368.

Razavi, S. H., Blanchard, F., & Marc, I. (2006). UV–HPLC/APCI MS method for separation and identification of the carotenoids produced by *Sporobolomyces ruberrimus* H110. *Iranian Journal of Chemistry & Chemical Engineering*, *25*, 1–10.

Rodea-González, D. A., Cruz-Olivares, J., Román-Guerrero, A., Rodríguez-Huezo, M. E., Vernon-Carter, E. J., & Pérez-Alonso, C. (2012). Spray-dried encapsulation of chia essential oil (*Salvia hispanica* L.) in whey protein concentrate-polysaccharide matrices. *Journal of Food Engineering*, *111*(1), 102–109.

Román-Guerrero, A., Orozco-Villafuerte, J., Pérez-Orozco, J. P., Cruz-Sosa, F., Jimenez-Alvarado, R., & Vernon-Carter, E. J. (2009). Application and evaluation of

mesquite gum and its fractions as interfacial film formers and emulsifiers of orange peel oil. *Food Hydrocolloids*, *23*(3), 708–713.

Ruíz-Ramos, J. O., Pérez-Orozco, J. P., Báez-González, J. G., Bósquez-Molina, E., Pérez-Alonso, C., & Vernon-Carter, E. J. (2006). Interrelationship between viscoelastic properties and effective moisture diffusivity of emulsions with the water vapor permeability of edible films stabilized by mesquite gum–chitosan complexes. *Carbohydrate Polymers*, *64*(2), 355–363.

Samavati, V., Emam-Djomeh, Z., Mohammadifar, M. A., Omid, M., & Mehdinia, A. (2011). Influence of tragacanth gum exudates from specie of *Astragalus gossypinus* on rheological and physical properties of whey protein isolate stabilised emulsions. *International Journal of Food Science and Technology*, *46*, 1636–1645.

Samavati, V., Emam-Djomeh, Z., Mohammadifar, M. A., Omid, M., & Mehdinia, A. L. I. (2012). Stability and rheology of dispersions containing polysaccharide, oleic acid and whey protein isolate. *Journal of Texture Studies*, *43*, 63–76.

Shih, C. K., Chang, J. H., Yang, S. H., Chou, T. W., & Cheng, H. H. (2008). β-Carotene and canthaxanthin alter the pro-oxidation and antioxidation balance in rats fed a high-cholesterol and high-fat diet. *Journal of Nutrition*, *99*, 59–66.

Sila, D. N., Van Buggenhout, S., Duvetter, T., Fraeye, I., De Roeck, A., Van Loey, A., et al. (2009). Pectins in processed fruits and vegetables: Part II-structure function relationships. *Comprehensive Reviews in Food Science and Food Safety*, *8*(2), 86–104.

Sun, C., & Gunasekaran, S. (2009). Effects of protein concentration and oil-phase volume fraction on the stability and rheology of menhaden oil-in-water emulsions stabilized by whey protein isolate with xanthan gum. *Food Hydrocolloids*, *23*, 165–174.

Sun, C., Gunasekaran, S., & Richards, M. P. (2007). Effect of xanthan gum on physicochemical properties of whey protein isolate stabilized oil-in-water emulsions. *Food Hydrocolloids*, *21*, 555–564.

Taherian, A. R., Britten, M., Sabik, H., & Fustier, P. (2011). Ability of whey protein isolate and/or fish gelatin to inhibit physical separation and lipid oxidation in fish oil-in-water beverage emulsion. *Food Hydrocolloids*, *25*, 868–878.

Wang, B., Wang, L. J., Li, D., Adhikari, B., & Shi, J. (2011). Effect of gum Arabic on stability of oil-in-water emulsion stabilized by flaxseed and soybean protein. *Carbohydrate Polymers*, *86*, 343–351.

Yue, P. F., Lu, X. Y., Zhang, Z. Z., Yuan, H. L., Zhu, W. F., Zheng, Q., et al. (2009). The study on the entrapment efficiency and *in vitro* release of puerarin submicron emulsion. *American Association of Pharmaceutical Scientists, AAPS PharmSciTech*, *10*(2), 376–383.